

Printability and mechanical properties of wood resin polymer composites manufactured using stereolithography

Oladayo Ariyo[†]

Graduate Student
Department of Applied Engineering Technology
North Carolina Agricultural and Technical State University,
Greensboro, North Carolina, U.S.A.
E-mail: oariyo@aggies.ncat.edu

Wenjia Wang

Assistant Professor
Department of Wood Science and Engineering,
Oregon State University
Corvallis, Oregon, U.S.A
E-mail: wenjia.wang@oregonstate.edu

James D. Kribs

Assistant Professor
Department of Applied Engineering Technology
North Carolina Agricultural and Technical State University
Greensboro, North Carolina, U.S.A
E-mail: jdkribs@ncat.edu

Aixi Zhou^{*}

Vice Provost of Research and Innovation; Professor of Engineering
Norfolk State University
Norfolk, Virginia, U.S.A
E-mail: azhou@nsu.edu

(Received 24 September 2024)

Abstract. Wood polymer composites (WPC) fabrication using stereolithography has received little attention. WPC research has been mostly directed to traditional manufacturing methods and fused deposition modeling. Stereolithography offers better print precision, structural accuracy, and ease of production than other 3D printing methods and directly creates the final wood polymer composite. Typically, WPCs fabricated using traditional methods used 40-60% wood in the mixture; however, the highest ratio used with stereolithography has been 10%. Increased wood content reduces costs and creates a product that more closely resembles the mechanical properties of wood. This study focused on increasing the wood flour ratio of WPC printed using stereolithography beyond 10% while studying the factors influencing printability and the mechanical properties of the printed materials. A blend of maple and oak wood flour was combined with methacrylate-based resin at wood levels of 2.5, 5, 7.5, 10, 12.5, 15, and 17.5 wt. % to fabricate the wood polymer composite. The highest ratio of wood flour successfully printed in this study was 17.5 wt.%. This paper discusses the tensile and compressive behaviors of the WPC, as well as the dimensional accuracy of the stereolithography process for higher wood ratio WPC fabrication. The process of fabrication, post processing, success and failure in printing, and characterization of print defects were also studied. Stereolithography can be used to manufacture wood polymer composites in a direct production method at higher wood flour ratios, and improving the capability of the method holds the potential to increase access to a sustainable substitute for conventional wood for various uses.

Keywords: Wood, Wood Polymer Composite, 3D Printing, Stereolithography, Sustainability

Introduction

The growing need for sustainable composite materials has spurred interest in pairing wood and other natural fibers with polymers. Wood, renowned for its specific strength, stiffness,

biodegradability, and non-abrasive nature, is particularly appealing as a reinforcing material (Bledzki et al. 2005; Nachtigall et al. 2007). The use of natural fibers in this capacity has witnessed substantial growth in recent years, due to advantages such as lower production cost, density, ease of preparation, and reduced energy requirements for processing (Baley 2002; Bledzki 1999; Oksman et al. 2003; van Voorn et al. 2001). Wood polymer composite or wood plastic composite (WPC)

^{*} Corresponding author

[†] Society of Wood Science & Technology member

are materials generated from the amalgamation of wood-derived elements like sawdust or lumber fibers with polymers to produce a composite material (Gardner et al. 2015; Schwarzkopf and Burnard 2016). These composites exhibit improved mechanical properties, moisture resistance, biological resistance and high molding performance (Huang et al. 2021). Given the different anatomical structures of various wood species, and the chemical structure of polymers, a blend of both produces distinct physical, thermal, and mechanical properties, paving the way for a new generation of hybrid materials (Youngquist et al. 1994). Wood fibers contribute to the composite's overall strength and stiffness, while the polymer matrix binds it together and provides flexibility (Faruk et al. 2012; Peltola et al. 2014). Strength and stiffness are essential properties in architectural applications, ensuring structural integrity and durability. Conversely, materials with high compliance provide flexibility and adaptability, making them ideal for applications requiring resilience and the ability to deform under stress without sustaining permanent damage. Composites that balance these attributes have significant potential in various applications, including flooring and other architectural elements. Custom furniture, decorative paneling, fences, and decking. In the automotive industry, Stereolithography -printed WPCs can be used for interior components such as dashboard panels, trim, and other decorative elements (Krapež Tomec and Kariz 2022). Other areas of use can be found in art installations, prototyping, and consumer goods manufacturing (Khan et al. 2020).

Stereolithography (SLA) outperforms other 3D printing methods for WPCs when considering ease of production, print precision and build resolution (Wang et al. 2017). The print precision of SLA improves structural accuracy, making it a viable development technique for WPC (Chan et al. 2018). SLA is a vat-polymerization technique that utilizes UV light in a layer-by-layer photopolymerization process to selectively cure liquid resin, transforming it into a solid three-dimensional structure (Bártolo 2011; Schmidleithner and Kalaskar 2018), which is illustrated in Figure 1. Objects created through this approach have gained widespread popularity and are used across various industries including automotive, architecture, and medicine (Dizon et al. 2021; Schmidleithner and Kalaskar 2018). Thermoset polymers like epoxy, polyvinyl ester, polyester, polyurethanes, and phenolics are employed in SLA, and have been used for fabricating polymer composites. Epoxy resin is commonly favored for composite development due to numerous advantages including high interfacial adhesion with fillers, low viscosity, enhanced wettability, thermal stability, superior mechanical performance, minimal shrinkage after

curing, and improved chemical resistance (Khan et al. 2020; Shi et al. 2017).

A variety of wood-based materials such as lignin, sawdust, and wood powder can be utilized in SLA-based 3D printing to create wood polymer composites with enhanced mechanical and physical properties. SLA allows particle reinforcements to be easily added (Yao and Hakkarainen 2023). In one study, Zhang et al. (2019) used a softwood kraft lignin as a filler in SLA 3D printing to reinforce the mechanical properties of printed products. Tensile testing revealed that adding lignin to the composite increased the tensile strength by 46–64% and the Young's modulus by 13–37% compared to the control sample (without lignin). Incorporating 0.4 wt. % softwood kraft lignin resulted in the printed composite achieving its highest tensile strength of 49.0 MPa, which represented a 60% increase in comparison to the control. Sutton et al. (2018) produced resins containing up to 15% lignin that displayed outstanding printing quality, strong layer fusion, high surface definition, and visual clarity. They reported that the ductility of printed parts rose with increased lignin concentration. Vidakis et al. (2022) also reinforced a medical-grade UV-cured resin (BioMed Clear) used in SLA 3D printing with cellulose nanofiber nanocomposites at concentrations ranging from 0.5 wt.% to 2.0 wt.%. They found improved mechanical properties, even at fractions as low as 0.5 wt.%. Tensile strength rose from 24.89 MPa (pure resin) to 50.25 MPa (Biomed Clear / cellulose nanofiber blend (CNF) 1.0 wt.%). Even greater improvements were observed for the flexural properties where the flexural strength increased by over 300% for the Biomed Clear CNF 0.5 wt.% (Vidakis et al. 2022). The incorporation of wood-derived reinforcements like wood flour/particles, lignin, and cellulose nanofibers into SLA resins can enhance tensile strength, modulus, and impart unique wood-like characteristics to the printed composites. Specific property values depend on the resin formulation and wood reinforcement type/loading, but the results show the potential for integrating wood flour into resins for fabricating wood polymer composites.

WPC properties vary depending on the type of wood, polymer, processing methods, and additives (Anish et al. 2023). Other notable factors influencing WPC properties are the shape, size and proportion of wood particles. The proportions of wood flour mixed with polymer have a considerable impact on both the processing and end-use properties. For instance, Huang et al. (2021) discovered that the tensile strength of 3D printed WPCs using fused deposition modeling (FDM) increased by 27% with the addition of wood components ranging from 19 wt.% to 29 wt.%. Kariz et al. (2018) found that up to

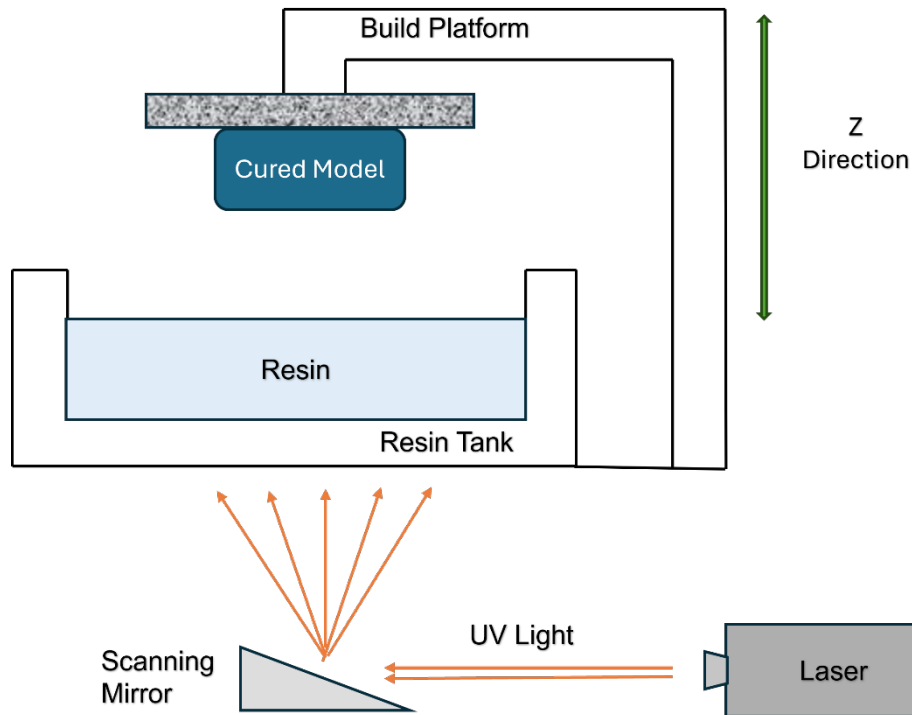


Figure 1. A schematic diagram of the process of stereolithography.

10% of wood particles slightly reinforced a WPC filament used in FDM 3D printing, but higher wood levels decreased tensile strength. Chaudemanche et al. (2018) observed that both bending strength and modulus rose with increased wood powder particle concentration. Higher wood ratios have other benefits brought about using less polymer (Sommerhuber et al. 2017). More wood enhances the physical appearance of the composite, making it resemble actual wood, and increasing its wood-like characteristics, while lowering production cost, since it is cheaper to use more wood and less resin (Fu et al. 2022; Pringle et al. 2017). Higher wood concentrations enhance hardness, while increased plastic matrix augments the toughness of the composite material (Jian et al. 2022). To maximize these benefits, it is preferable to have a high wood flour content, typically 50 wt.% or higher in traditional methods. Commercial WPC products typically utilize wood flour contents of up to 70% (Matuana and Stark 2015). However, increased filler amounts significantly raise the viscosity of the polymer melt, making flow and forming processes more challenging (Mazzanti and Mollica 2020). Wood species used for reinforcement are based on availability and ease of access rather than on characteristics (Tanaka and Ito 2013). Hemp, ramie, and kenaf are utilized as fillers in Southeast Asia due to their abundance. Conversely softwoods such as white pine, spruce, and hemlock, as well as hardwoods like aspen, oak,

and maple are the primary species employed in the US as fillers (Clemons 2008; Clemons and Caulfield 2005; Pokhrel et al. 2021). Berger and Stark (1997) revealed that hardwood species offer enhanced tensile properties and superior heat deflection in comparison to softwoods.

Limited research has been done on the behavior of WPCs fabricated using SLA at high wood flour ratios (e.g., 10 wt.% or higher). Zhang et al. (2021) successfully used SLA to fabricate WPCs at ratios ranging from 1 to 10 wt.%. Their addition of 1% poplar wood flour to methacrylate resin greatly improved the tensile strength and Young's modulus of the printed WPCs. The purpose of this current study was to fabricate WPCs using SLA at ratios higher than 10 wt.% using a 1:1 oak/maple wood flour blend. Oak and maple were chosen due to their high cellulose content which improves structural properties of wood. Increased wood flour content will enhance the suitability of SLA for fabricating WPCs for commercial purposes.

Materials and methods

Wood flour (Fasco Epoxies, Fort Pierce, FL, USA), was a blend of two hardwoods, Maple, and Oak. The particle size of the wood flour was 80 mesh (177 μm). The wood flour was dried at 103°C for 24 hours, resulting in a measured moisture content of 3%, as determined by a Reed dual moisture meter.

The thermoset resin used in this study was RS-F2-DUCL-02 (Formlabs Inc., Sommerville, MA USA) with a density of 1.06 g/cm³. The resin formulation contained methacrylic acid esters, photo-initiators, proprietary pigment, and additive packages, with viscosities of 2051 and 981 cp at 25 and 35°C, respectively.

The 3D printer used was a Formlabs Form 3 printer (Formlabs Inc., Sommerville, MA USA) with a preset UV light wavelength of 405 nm. Isopropyl alcohol, utilized for washing purposes, was procured from USA Lab, (Livonia, MI, USA). Additionally, a UV curing chamber and wash basin were obtained from Formlabs Inc.

STL files containing models of ASTM D695 and ASTM D638 Type V were generated using AutoCAD Fusion 360 and sliced using Formlabs Preform slicing software before being uploaded to the 3D printer. The layer height of each print was set at 0.1 mm, and a default build orientation of 0 degrees was chosen. The wood flour and resin were manually mixed at room temperature (25°C) until a consistent blend was obtained. This method was used to prevent phase separation while being held in any containers. The resin was not diluted because its viscosity was considered an integral factor in procuring increased wood flour ratios. Hand stirring was found to be the best form of blending due to the increased viscosity of the resin. Resin (300 g) was measured for the printing process; the wood flour was divided into 2.5 wt.% increments were added to the resin

to levels of 5, 7.5, 10, 12.5, 15 and 17.5 wt.%. The control samples with dimensions can be seen in Figure 2.

The wood-polymer blend was added to the resin tank and printing commenced at 35°C. Samples were fabricated based on ASTM standards D638 Type V (tensile coupon) and D695 (compression coupons). Fabrication of ten samples was attempted at each ratio for both ASTM standards. After printing, the successful samples were moved to an isopropyl alcohol wash station for 20 minutes to remove excess resin. The samples were then cured in a UV chamber for 60 minutes at 60°C. The dimensions of all samples were measured using an Insize 1114-150A digital caliper to determine accuracy. A summary of the printed samples is in Table 1. Samples were given specimen IDs for easy identification. Scanning electron microscopic imaging was performed using a Zeiss Evo LS Environmental SEM to observe the surface and microstructure of the WPCs. The dimensional accuracy of the samples was determined using a vernier caliper, as part of the study on printability, while failure modes observed during the printing process were also identified and recorded.

Mechanical testing

Tensile testing was conducted at room temperature (25°C) using an Instron 5969 universal testing machine (Instron, Norwood, MA, USA) following the guidelines outlined in ASTM D 638: Standard Test Method for Tensile Properties of Plastics.

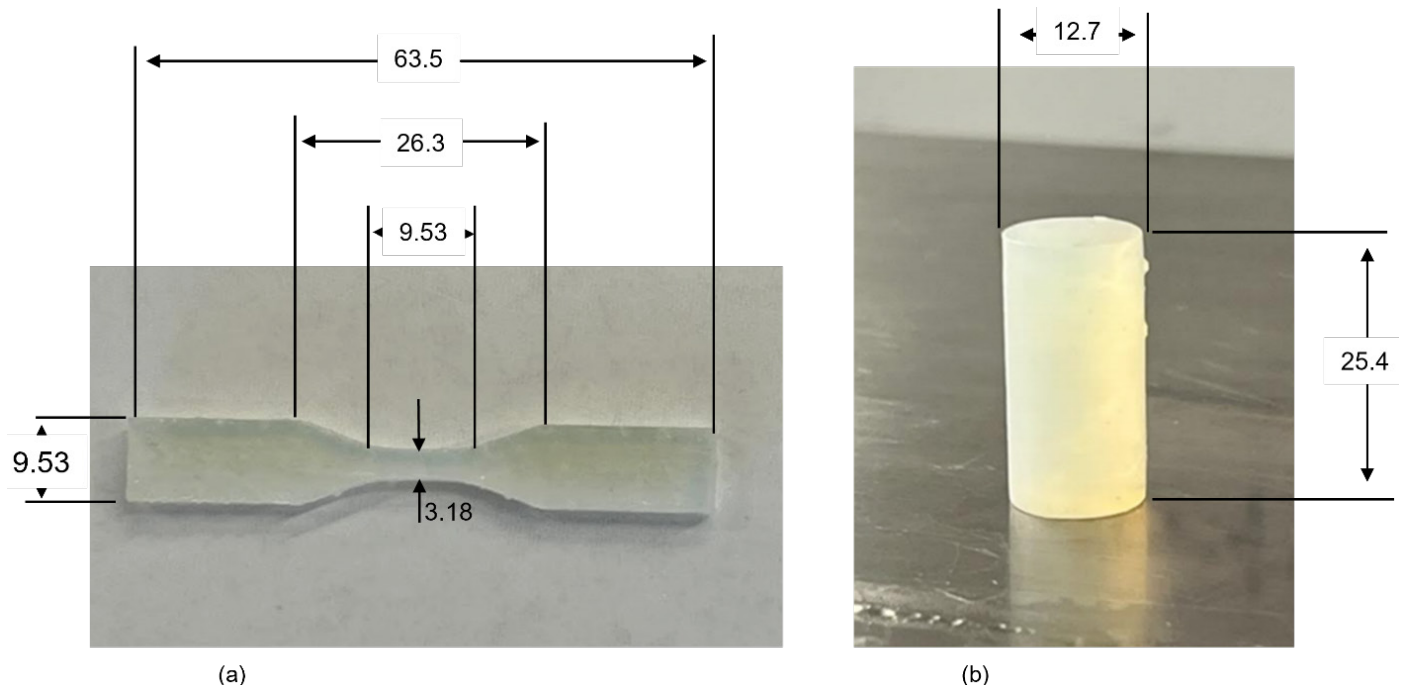


Figure 2. Examples of test specimens used for (a) WPC1 ASTM D638 and (b) WPC1 ASTM D695. Measurements in mm.

Table 1. Effect of wood flour content on ability to produce acceptable specimens for ASTM Standards D638 and D695.

wt.% Wood Content (nominal)	Specimen ID	wt.% Wood Content (measured) Ave. \pm S.D	Number of Successful D638 Specimens	Number of Successful D695 Specimens
0.0	WPC1	0.00	10	10
2.5	WPC2	2.65 \pm 0.11	10	10
5.0	WPC3	5.30 \pm 0.21	10	8
7.5	WPC4	7.95 \pm 0.32	10	8
10.0	WPC5	10.60 \pm 0.42	10	9
12.5	WPC6	13.25 \pm 0.53	10	8
15.0	WPC7	15.90 \pm 0.64	10	9
17.5	WPC8	18.55 \pm 0.74	7	4

Compression testing followed the guidelines outlined in ASTM D 695: Standard Test Method for Compressive Properties of Rigid Plastics. The load cell had a capacity of 50 KN, and the crosshead speed was 1 mm/min for tensile testing and 2.5 mm/min for compression testing. Seven samples were used for tensile testing, while five samples were used for compression testing (except WPC8 with only four specimens). The reduced replication reflected printing failures that precluded testing.

Results and discussion

The ASTM D638 and D695 coupons were successfully fabricated at increased wood flour content higher than 10 wt. % when blended with epoxy resin, with both sample types peaking at 17.5 wt.% of wood flour. Samples did not fully form the intended model and did not print when 20 or 22.5% wood flour was added, at all respectively. This was attributed to decreased melt flow and increased viscosity of the resin mixture upon high wood flour addition. A reduction in UV light penetration was observed, and without the curing, laser print failure was inevitable. The wood flour darkened the printed polymer composite samples, and an increasing darkness was observed as the wood ratio increased (Figure 3). The texture of the composites was grainier at higher wood content above 12wt.%, particularly with the cylindrical shaped samples. This was attributed to the uneven shape of the wood particles and the continuous redistribution of wood flour during the printing process due to the movement of the build plate. Both sample types showed a distinct color change due to increased wood content. Figure 4 shows the SEM of wood flour particles suspended within the matrix of a WPC8 sample. Uniform distribution and alignment of wood fibers within the polymer matrix are critical for maximizing tensile strength. This uniform distribution was not guaranteed in this process due to the movement of the build plate.

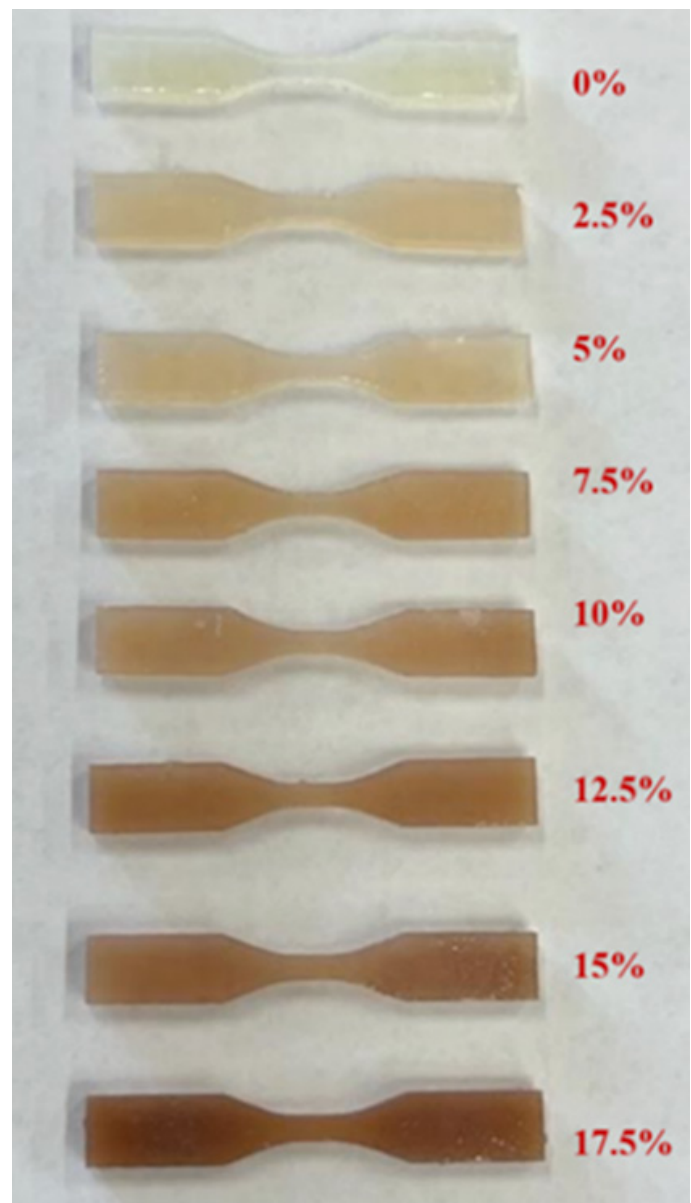


Figure 3. Color gradient changes observed in tensile coupons with increased wood flour content (wt. %).

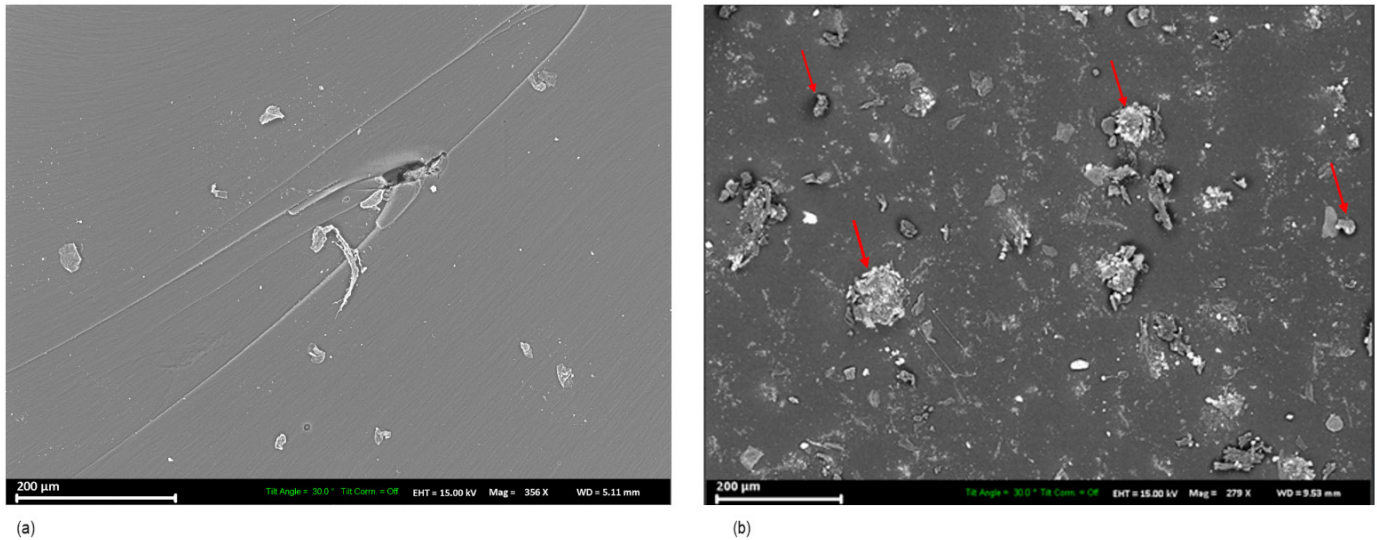


Figure 4. SEM images of cross sections of tensile coupons with (a) no wood and (b) 17.5 wt.% wood showing wood flour dispersion. The white circles in image (b) are suspended wood flour.

Printability

Printability is an important consideration in various printing processes, including offset and digital printing. In 3D printing, printability pertains to the final appearance and structural accuracy of the printed materials. Good printability characteristics yield high-quality, dimensionally accurate, and visually appealing results. Considerations given to printability in this paper are important because wood polymer fabrication using SLA is less common and requires more process clarity. Printability will be discussed in terms of the success and failure of the samples and dimensional accuracy. A successful sample was categorized as one that was fully printed with accurate dimensions within allowed tolerances (measured using a vernier caliper), had little to no surface roughness and high print resolution. Failed samples were classed as samples fabricated with deformities, inaccurate dimensions, and incomplete curing (undeveloped features). As shown in Table 1, ASTM D638 coupons with 2.5 to 15 wt.% of wood flour ratio were 100% successful, while the samples with 17.5 wt.% had a 70% success rate (7 of 10). The ASTM D695 coupons showed more variance in success. The 2.5 wt.% ratio was 100% successful, 10 and 15 wt.% ratios were 90% (9 of 10) successful, and 5, 7.5 and 12.5 wt.% were 80% successful (8 of 10), while 17.5 wt.% showed the lowest success rate at 40% (4 of 10). Major printing factors that affect print success in stereolithography are intensity of laser power, layer height, print speed, curing time and printing resolution (Wang et al. 2017; Mohammadzadeh and Fidan 2021)

Dimensional accuracy

Dimensions for the cylindrical (ASTM D695) and dog-bone (ASYM D638) test specimens were measured to study fabrica-

tion accuracy. All measurements were performed thrice using a digital caliper. For the cylindrical coupon, diameter and length were measured, while for the dog-bone coupon, width and thickness of the gauge section were measured. The graphs in Figure 5 show the dimensions of length and diameter of the compression coupon, as compared to the no wood control. Figure 6 shows the thickness and width measurements of the tensile coupon as compared to the control. The dimensional deviations observed in the compression samples were 0.076 mm for width and 0.154 mm for thickness. For the tensile coupons, the deviations were 0.421 mm for length and 0.145 mm for diameter. Insufficient compatibility between the polymer and wood fibers can result in weak interfaces, leading to uneven shrinkage during cooling. In addition, some polymers used in WPCs exhibit significant shrinkage during solidification, exacerbating dimensional inaccuracies. Further study of the polymer feedstock could improve our understanding of this phenomenon. Polymerization shrinkage affects the final dimensions of composites when monomers pack closer together during the polymerization process (Schricker 2017).

Printing failure modes

The failure modes observed during printing were categorized and documented for similarities; this was used to identify several types of defects present in wood polymer composite fabrication using stereolithography. Those listed here do not represent an exhaustive list but are the defects observed during this experiment.

- *Non-Adherence* is when the part partially or fully detached from the build plate before print completion.

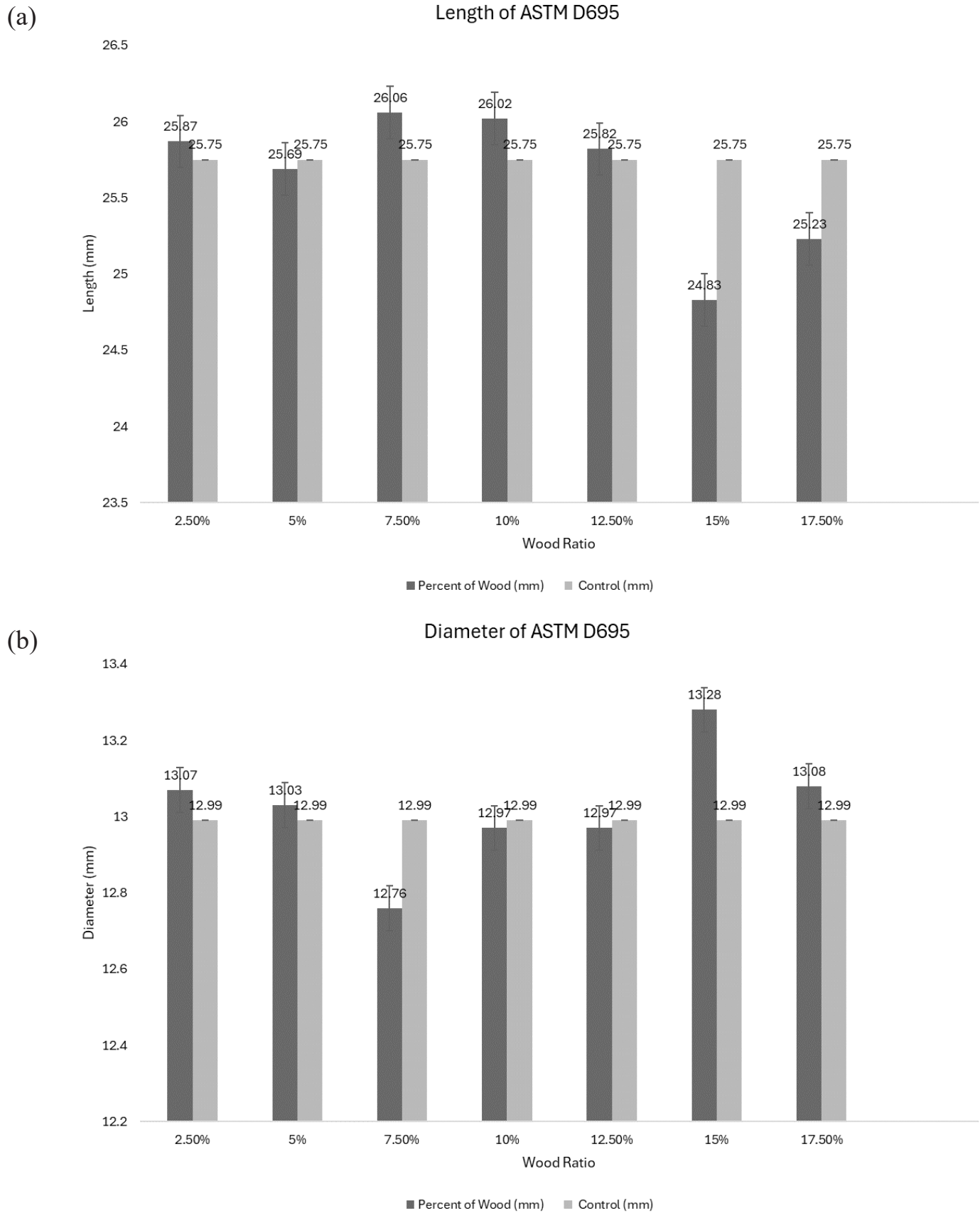
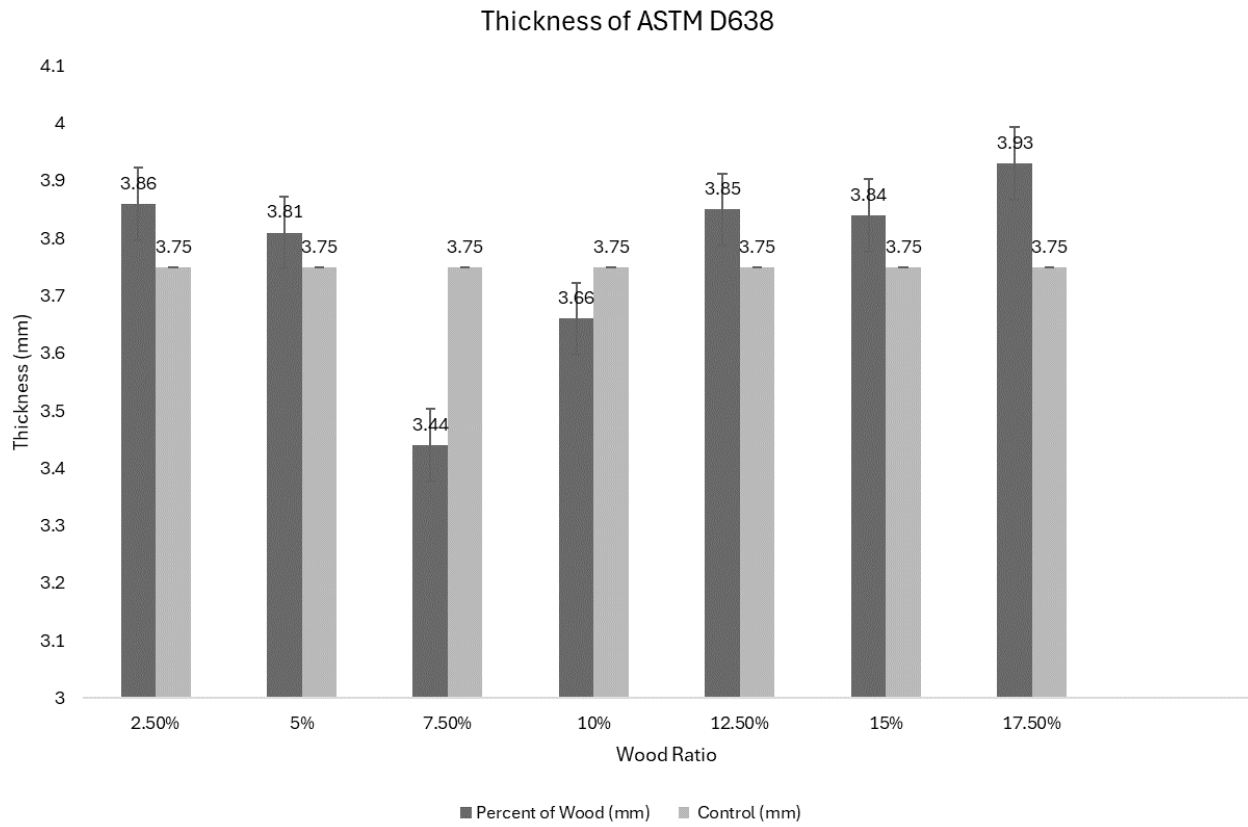


Figure 5. Effect of increased wood flour addition on (a) ASTM D695 cylinder length and (b) ASTM D695 cylinder diameter. Error bars represent one standard deviation.

(a)



(b)

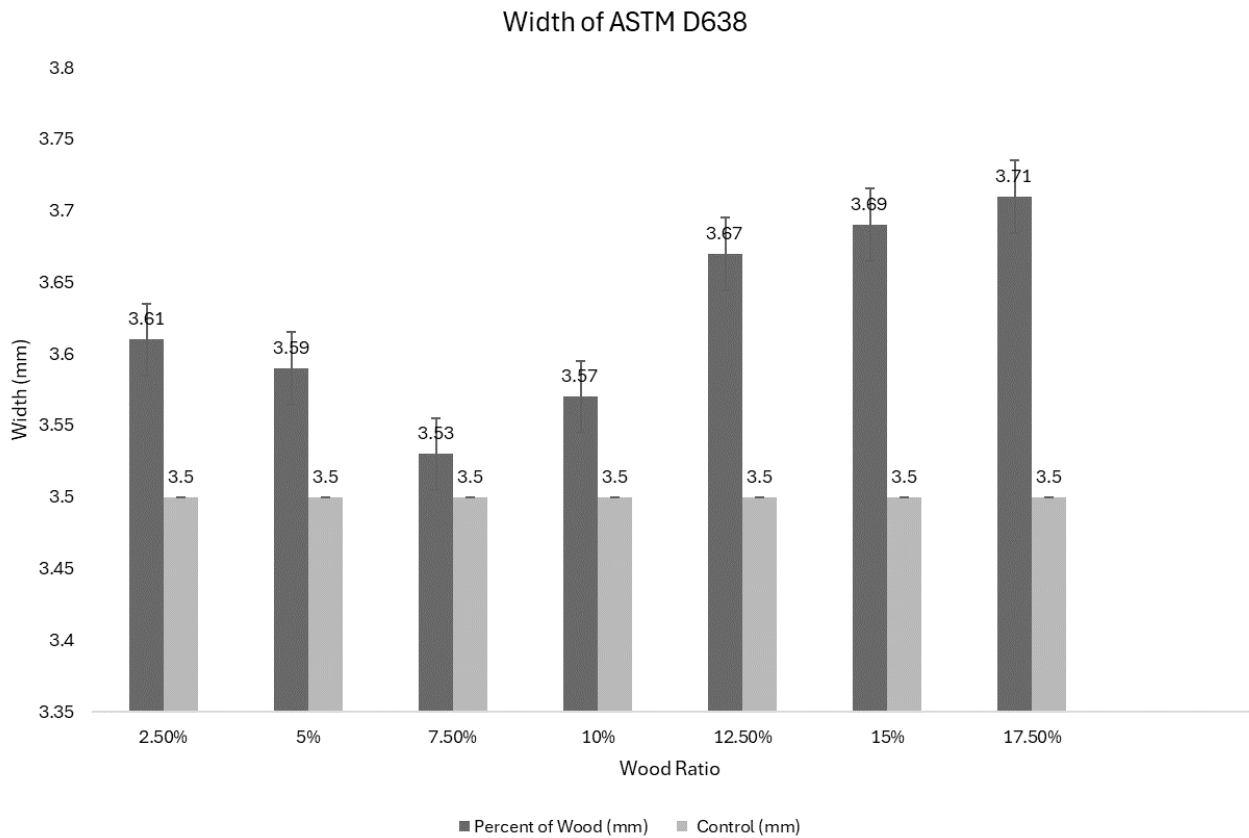


Figure 6. Effect of increased wood flour addition on (a) ASTM D638 dog-bone thickness (b) ASTM D638 dog-bone width. Error bars represent one standard deviation.

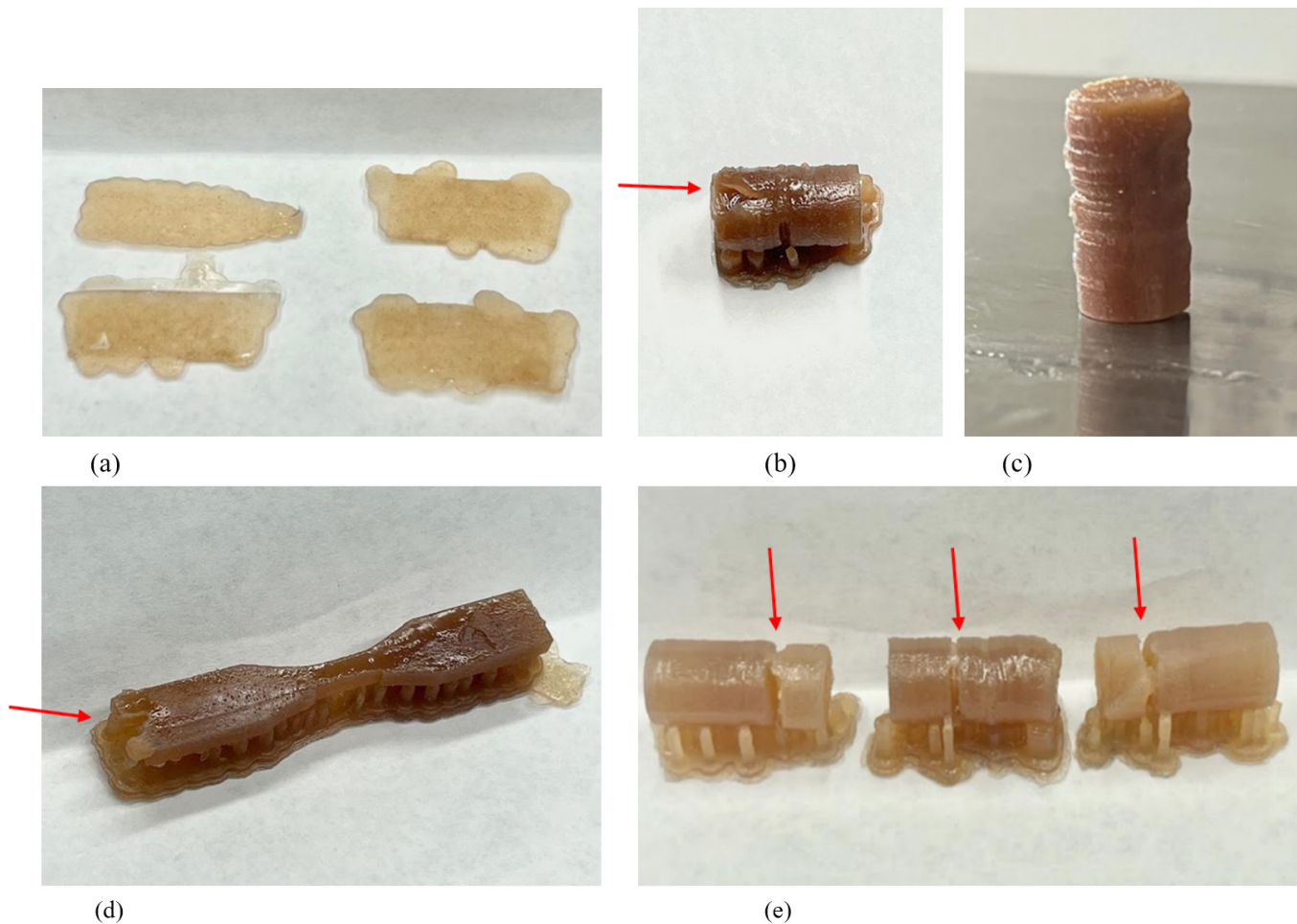


Figure 7. Examples of defects observed in the fabrication of 3D printed WPC samples. (a) Raft silhouettes observed in ASTM D695 that occur when the first printed layer sticks to the build plate but preceding layers do not adhere (b) Cuts observed in 17.5 wt.% woodflour ASTM D695 coupons (c) Surface roughness observed in 17.5 wt.% wood flour sample (d) Incomplete curing at the edge of a 17.5 wt.% wood flour ASTM D638, (e) Pinholes and cuts observed in 10.0 wt.% and 12.5 wt.% wood flour ASTM D695 coupons.

- **Raft Silhouetting** occurred when the first layer of the print stuck to the build plate, but the preceding layers did not adhere, resulting in a failed print for that sample. This can also occur when the first layer sticks to the base of resin tank, as in bottom-up 3D printers and the preceding layers do not adhere (Figure 7a). This was observed at higher wood flour ratios. This can be attributed to wood flour clouding the resin tank and restricting UV light penetration (Formlabs Inc 2023).
- **Incomplete Curing and Dimensional Inaccuracy** occurred when inadequate polymer curing resulted in a distortion in the sample shape resulting in undeveloped features and an incomplete print. This was due to potential variations in layer thickness and curing behavior (Figure 7d).
- **Pinholes and Cuts** occurred when a void formed around the print and can take the form of a hole, ridge or slit that extends from one side of the part to another (Formlabs Inc 2023). (Figure 7b and 7e).
- **Poor Surface Quality and Warping:** SLA-printed surfaces can exhibit roughness and layering artifacts, (Figure 7e). Samples fabricated with these defects may need post-processing to achieve a smooth finish in wood polymer composites (Figure 7c).
- **Delamination:** Layer-by-layer deposition in SLA can result in poor adhesion between the printed layers of wood-polymer composite, leading to delamination issues. This is related to increased viscosity of the resin and layer thickness (Formlabs Inc 2023).

The data showed that as the wood flour content increased the success of sample fabrication decreased for both sample types. This directly impacts printability and could be attributed to a few factors that will now be discussed.

Tensile performance

Tensile strength for each sample was identified by locating the peak stress value on the stress-strain graph. Young's modulus

was calculated by analyzing the linear segment within the designated strain interval on the same curve in the range of 0–0.2. The tensile stress and the Young's modulus for each composite were obtained from the average of five samples (Figures 8 and 9). Tensile strength of WPC1 (the control) was 22.1 MPa, and increased by 2 % to 23.1 MPa with the addition of 2.5 wt.% of wood flour, while Young's modulus decreased from 860.1 MPa to 842 MPa with the same level of wood flour addition. Tensile strength increased 8% with the addition of another 2.5 wt. % of wood flour in WPC3 coupled with an increase in Young's modulus to 895 MPa.

Further additions of wood flour resulted in decreasing tensile strength, WPC4 and WPC5 showed similar tensile strengths of 21.1 and 21.2 MPa respectively. WPC6 (12.5 wt.%) showed a further reduction in tensile strength to 20.2 MPa, while Young's modulus decreased to 663.3 MPa. However, 15 wt.% wood flour (WPC7) was associated with another increase in Young's modulus, rising to 730 MPa, albeit with a decline in tensile strength to 19.7 MPa. The final successful wood flour ratio of 17.5 wt.% experienced further reduction in tensile strength to 17.2 MPa and a Young's modulus of 501.4 MPa. The tensile performance confirmed results found by Zhang et al. (2021) and Feng et al. (2018) that low levels of wood flour

can reinforce SLA fabricated polymer composites (Zhang et al. 2021). The result also shows that continuous increase in wood flour content will reduce tensile strength and Young's modulus of wood polymer composites. The moderate rise in tensile strength and Young's modulus at low levels of wood flour addition suggests that the composites have high stiffness and are resistant to (elastic) deformation when subjected to load. The tensile performance of SLA-printed WPCs was comparable to those manufactured through traditional methods, such as extrusion or compression molding (Nukala et al. 2022). Uniform distribution and alignment of wood fibers within the polymer matrix are critical for maximizing tensile strength. Ensuring fibers are well-aligned along the load direction can significantly enhance the tensile properties of WPCs.

Compression performance

The ultimate compressive strength was calculated using the equation:

$$F = P / A \quad (1)$$

where (F) is the compressive strength of the specimen in megapascals, (P) is the maximum applied load in newtons, and (A) is the cross-sectional area measured in square millimeters.

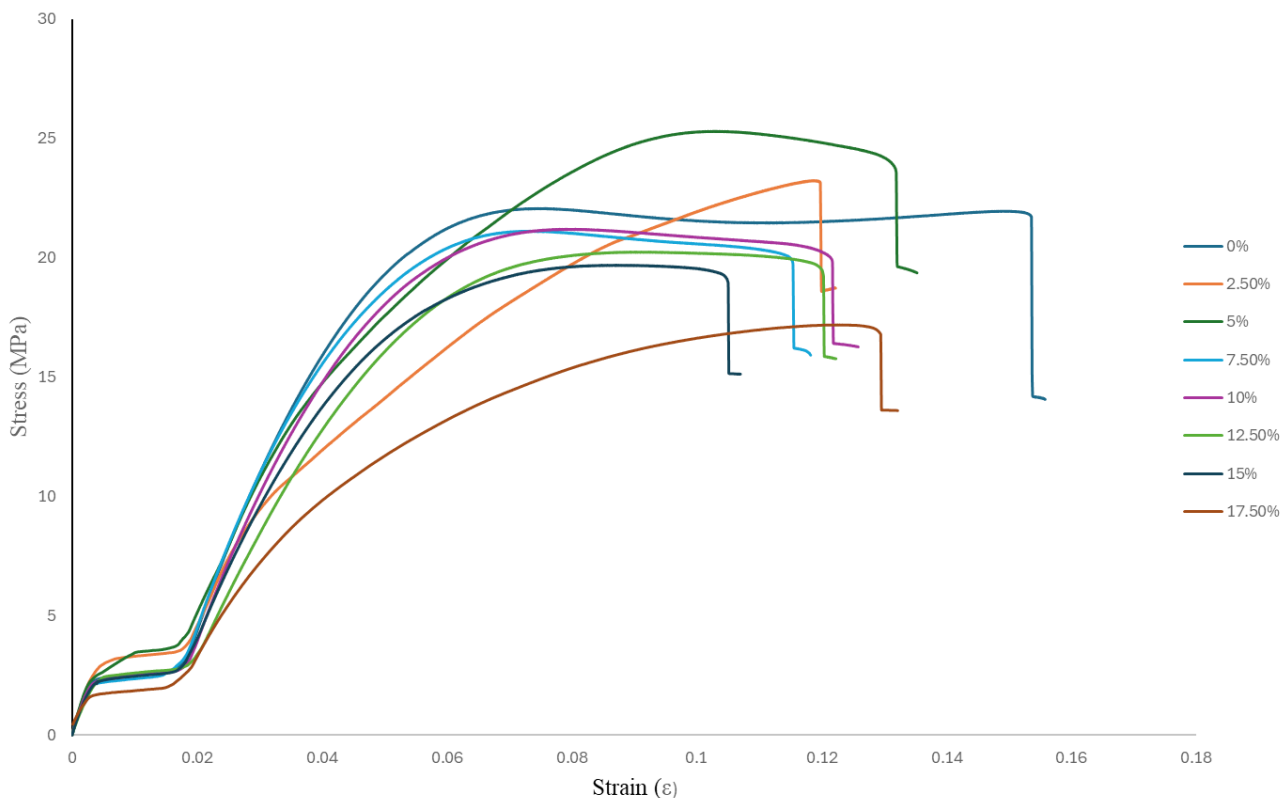


Figure 8. Examples of stress/strain plots for samples as wood flour levels increased from 0 to 17.5 wt.%.

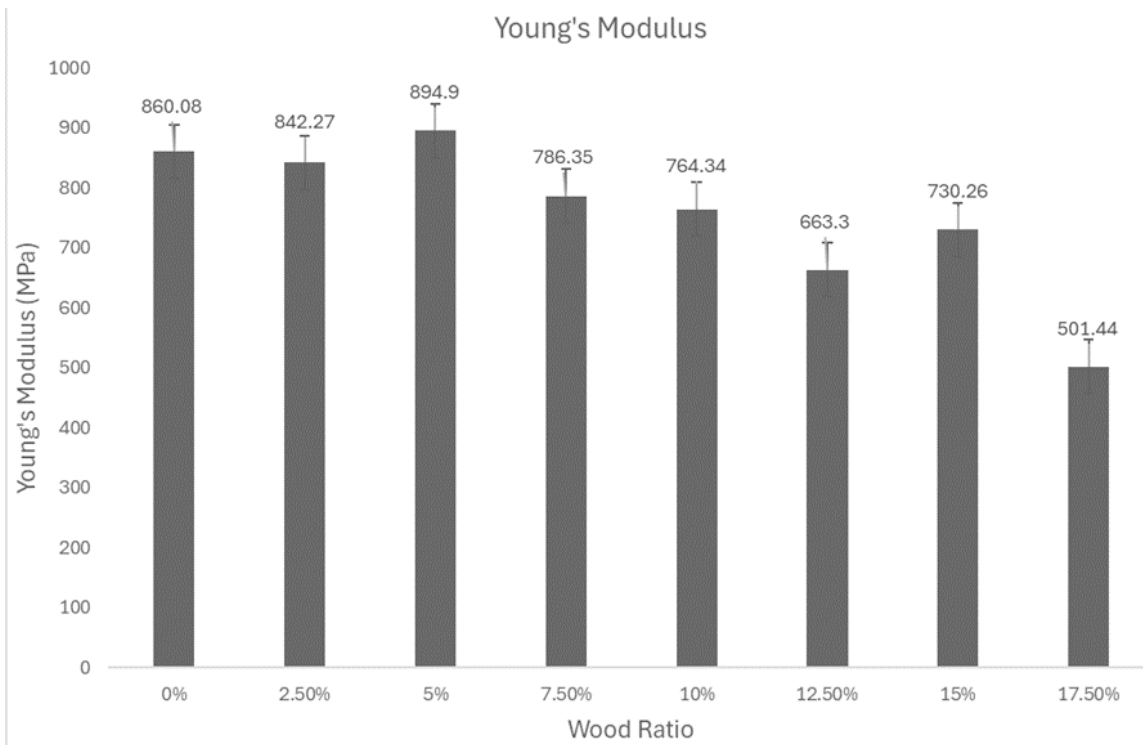


Figure 9. Effect of increasing amounts of wood flour from 0 to 17.5 % on Young's Modulus. Error bars represent one standard deviation.

WPC1 had a compressive strength of 22.3 MPa, WPC 2 was 29.8 MPa, and WPC3 increased significantly to 75.6 MPa. The increased compressive strength could be because of strain hardening, where a material becomes stronger and harder as it undergoes plastic deformation. Microstructural changes such as phase transformation or grain refinement were also likely to have occurred. WPC4 and WPC5 both experienced reduced compressive strengths, while WPC6 showed an uptick in strength to 29.3 MPa. WPC7 returned to trend with a reduction to 22.4 MPa and compressive strength of WPC8 was 15.8 MPa which was the lowest value recorded. This sample also had liquid resin within the internal structure upon fracture after extensive loading, showing signs of incomplete internal curing.

Wood flour addition was associated with increased stiffness and rigidity in the composites as evidenced by the increased elastic modulus (Table 2). WPC 2–7 showed an increase in elastic modulus, with WPC3 being the highest recorded at 320.8 MPa. These levels would make them suitable for applications where stiffness is desired such as bridge construction and furniture. The following samples showed an increase in compressive strength compared to the control at 2.5 wt.%, 5 wt.% 7 wt.% 12.5 wt.% and 15wt.%. All of the treatments except WPC5 and WPC8 experienced increased tensile strength. Increased compressive strength showed that the materials had good load bearing capacity and could maintain their shape under substantial compressive force. The wood flour amended WPCs

Table 2. Effect of wood concentration on tensile and compression strength of a 3D printed composite.

Wood Content (wt.%, nominal)	Tensile Strength (MPa)	Compressive Strength (MPa)	Compressive Strain (mm/mm)	Elastic Modulus (MPa)
0.0	22.1 ± 0.60	22.3 ± 5.31	24.8 ± 0.49	215.0 ± 21.93
2.5	23.2 ± 1.38	29.8 ± 0.01	25.8 ± 0.22	282.1 ± 25.52
5.0	25.3 ± 2.86	75.6 ± 32.38	25.8 ± 0.22	320.8 ± 52.88
7.5	21.2 ± 0.04	23.5 ± 4.46	26.1 ± 0.43	264.3 ± 12.93
10.0	21.1 ± 0.11	20.4 ± 6.65	26.0 ± 0.36	289.7 ± 30.89
12.5	20.2 ± 0.74	29.3 ± 0.36	25.4 ± 0.06	244.9 ± 0.78
15.0	19.7 ± 1.10	22.4 ± 5.24	24.8 ± 0.49	216.0 ± 21.22
17.5	17.2 ± 2.86	15.2 ± 10.33	25.2 ± 0.21	135.3 ± 78.28

Values represent means of 7 to 10 replicates while +/- figures represent one standard deviation.

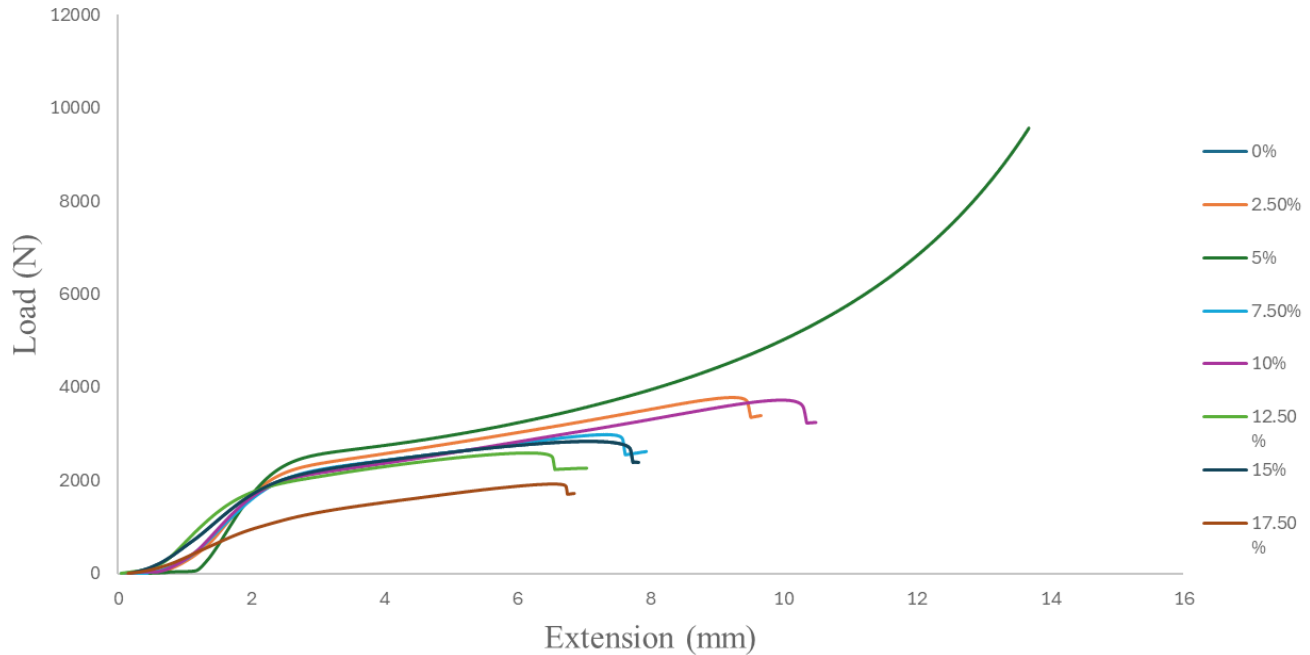


Figure 10. Compressive behavior of WPC with increased wood content.

exhibited superior compressive strength and stiffness compared to epoxy polymer at certain ratios (Figure 10). Strong interfacial bonding ensured efficient stress transfer from the matrix to the fibers, maximizing composite strength.

Conclusions

This study demonstrated printability and mechanical properties of WPC manufactured using stereolithography at wood content levels higher than 10%. Tensile and compressive mechanical tests were performed using printed WPC samples. The following statements summarize the main findings from the current study.

1. A limit of 17.5 wt.% wood flour content was determined to be the peak for the WPC using stereolithography when considering wood species, particle shape and size, density, resin viscosity and 3D printing capability.
2. Addition of 2.5 and 5.0 wt.% of wood flour increased the tensile strength of the composite before both properties declined with increasing wood flour content. WPCs exhibited enhanced tensile strength and stiffness due to the uniform dispersion of wood fibers within the polymer matrix and the ability to control layer-by-layer construction.
3. Young's modulus of the tensile samples increased at low wood flour ratios signifying reinforcement then decreased

with increased wood content. A slight increase was observed at 15.0 wt.% before further reductions were noted at 17.5 wt.%. Material stiffness was improved with 2.5 wt.% and 7.5 wt.% of wood flour, showing increased resistance to deformation and stiffness at those ratios.

4. Compressive strength increased at every ratio except 10 wt.% and 17.5 wt.%, indicating that the material had good load bearing capacity and could maintain its shape under substantial compressive forces. Elastic modulus also increased at all ratios except 17.5 wt.%, indicating an increase in stiffness and rigidity when wood flour was used to reinforce epoxy polymer.

Applications of SLA printed WPCs are diverse and span across various industries, from consumer products to advanced industrial components. Enhancing this method opens new opportunities for innovative and sustainable manufacturing solutions. Future research may focus on the printability of WPC using biodegradable resin as an alternative to petroleum-based feedstocks, the impact of particle size on printability and mechanical properties, and the dimensional accuracy of different print orientations.

References

- Anish MC, Pandey KK, Kumar R (2023) Transparent wood composite prepared from two commercially important tropical timber species. *Sci Rep* 13(1). <https://doi.org/10.1038/s41598-023-42242-7>

- Baley C (2002) Analysis of the flax fibres tensile behaviour and analysis of the tensile stiffness increase. *Compos Part A Appl Sci Manuf* 33(7):939–948. [https://doi.org/10.1016/S1359-835X\(02\)00040-4](https://doi.org/10.1016/S1359-835X(02)00040-4)
- Bártolo PJ (2011) *Stereolithography*. Springer US. <https://doi.org/10.1007/978-0-387-92904-0>
- Berger MJ, Stark NM (1997) Investigations of species effects in an injection-molding-grade, wood-filled polypropylene. *In: Proceedings of the Fourth International Conference on Wood Fiber-Plastic Composites*, 12–14 May; Madison, WI. pp. 19–25.
- Bledzki A (1999) Composites reinforced with cellulose-based fibres. *Prog Polym Sci* 24(2):221–274. [https://doi.org/10.1016/S0079-6700\(98\)00018-5](https://doi.org/10.1016/S0079-6700(98)00018-5)
- Bledzki AK, Letman M, Viksne A, Rence L (2005) A comparison of compounding processes and wood type for wood fibre-PP composites. *Compos Part A Appl Sci Manuf* 36(6):789–797. <https://doi.org/10.1016/j.compositesa.2004.10.029>
- Chan CM, Vandi LJ, Pratt S, Halley P, Richardson D, Werker A, Laycock B (2018) Composites of wood and biodegradable thermoplastics: a review. *Polym Rev* 58(3):444–494. <https://doi.org/10.1080/15583724.2017.1380039>
- Chaudemanche S, Perrot A, Pimbert S, Lecompte T, Faure F (2018) Properties of an industrial extruded HDPE-WPC: the effect of the size distribution of wood flour particles. *Constr Build Mater* 162:543–552. <https://doi.org/10.1016/j.conbuildmat.2017.12.061>
- Clemons C (2008) Raw materials for wood-polymer composites.
- Clemons CM, Caulfield DF (2005) Wood flour. *In: Functional Fillers for Plastics*. Wiley. pp. 249–270. <https://doi.org/10.1002/3527605096.ch15>
- Dizon JRC, Gache CCL, Cascolan HMS, Cancino LT, Advincula RC (2021) Post-processing of 3D-printed polymers. *Technologies* 9(3). <https://doi.org/10.3390/technologies9030061>
- Faruk O, Bledzki AK, Fink HP, Sain M (2012) Biocomposites reinforced with natural fibers: 2000–2010. *Prog Polym Sci* 37(11):1552–1596. <https://doi.org/10.1016/j.progpolymsci.2012.04.003>
- Feng C, Li Z, Wang H (2018) The effect of epoxy resin on wood-plastic composites. *Pigm Resin Technol* 47(5):369–376.
- Formlabs Inc. (2023) Diagnosing a print failure (SLA). https://support.formlabs.com/s/article/Diagnosing-a-print-failure?language=en_US
- Fu H, Dun M, Wang H, Zou C, Wang L, Zhou Z, Wang W, Xie Y, Wang Q (2022) Characterization of the structural rheological properties of wood flour-polyethylene composites with ultrahigh filling on the basis of uniaxial cyclic compression method. *Compos Part A Appl Sci Manuf* 153. <https://doi.org/10.1016/j.compositesa.2021.106724>
- Gardner DJ, Han Y, Wang L (2015) Wood-plastic composite technology. *Curr For Rep* 1(3):139–150. <https://doi.org/10.1007/s40725-015-0016-6>
- Huang Y, Lösckhe S, Proust G (2021) In the mix: the effect of wood composition on the 3D printability and mechanical performance of wood-plastic composites. *Compos Part C Open Access* 5. <https://doi.org/10.1016/j.jcomc.2021.100140>
- Jian B, Mohrmann S, Li H, Li Y, Ashraf M, Zhou J, Zheng X (2022) A review on flexural properties of wood-plastic composites. *Polymers* 14(19). <https://doi.org/10.3390/polym14193942>
- Kariz M, Sernek M, Obućina M, Kuzman MK (2018) Effect of wood content in FDM filament on properties of 3D printed parts. *Mater Today Commun* 14:135–140. <https://doi.org/10.1016/j.mtcomm.2017.12.016>
- Khan MZR, Srivastava SK, Gupta MK (2020) A state-of-the-art review on particulate wood polymer composites: processing, properties and applications. *Polym Test* 89. <https://doi.org/10.1016/j.polymertesting.2020.106721>
- Krapež Tomec D, Kariž M (2022) Use of wood in additive manufacturing: review and future prospects. *Polymers* 14(6). <https://doi.org/10.3390/polym14061174>
- Matuana LM, Stark NM (2015) The use of wood fibers as reinforcements in composites. *In: Biofiber Reinforcements in Composite Materials*. Elsevier Inc. p. 648–688. <https://doi.org/10.1533/9781782421276.5.648>
- Mazzanti V, Mollica F (2020) A review of wood polymer composites rheology and its implications for processing. *Polymers* 12(10):2304. <https://doi.org/10.3390/polym12102304>
- Mohammadizadeh M, Fidan I (2021) Tensile performance of 3D-printed continuous fiber-reinforced nylon composites. *J Manuf Mater Process* 5(3). <https://doi.org/10.3390/jmmp5030068>
- Nachtigall SMB, Cerveira GS, Rosa SML (2007) New polymeric-coupling agent for polypropylene/wood-flour composites. *Polym Test* 26(5):619–628. <https://doi.org/10.1016/j.polymertesting.2007.03.007>
- Nukala SG, Kong I, Kakarla AB, Tshai KY, Kong W (2022) Preparation and characterisation of wood polymer composites using sustainable raw materials. *Polymers* 14(15):3183. <https://doi.org/10.3390/polym14153183>
- Oksman K, Skrifvars M, Selin JF (2003) Natural fibres as reinforcement in polylactic acid (PLA) composites. *Compos Sci Technol* 63(9):1317–1324. [https://doi.org/10.1016/S0266-3538\(03\)00103-9](https://doi.org/10.1016/S0266-3538(03)00103-9)
- Peltola H, Pääkkönen E, Jetsu P, Heinemann S (2014) Wood based PLA and PP composites: effect of fibre type and matrix polymer on fibre morphology, dispersion and composite properties. *Compos Part A Appl Sci Manuf* 61:13–22. <https://doi.org/10.1016/j.compositesa.2014.02.002>
- Pokhrel G, Gardner DJ, Han Y (2021) Properties of wood-plastic composites manufactured from two different wood feedstocks: wood flour and wood pellets. *Polymers* 13(16). <https://doi.org/10.3390/polym13162769>
- Pringle AM, Rudnicki M, Pearce J, Wood JP, Pearce JM (2017) Furniture waste-based recycled 3D printing filament. *For Prod J* 68(1):10. <https://doi.org/10.13073/FPJ-D-17-00042>
- Schmidleithner C, Kalaskar DM (2018) *Stereolithography*. *In: 3D Printing*. InTech. <https://doi.org/10.5772/intechopen.78147>
- Schricker SR (2017) Composite resin polymerization and relevant parameters. *In: Orthodontic Applications of Biomaterials*. Elsevier. pp. 153–170. <https://doi.org/10.1016/B978-0-08-100383-1.00009-6>
- Schwarzkopf MJ, Burnard MD (2016) Wood-plastic composites—performance and environmental impacts. *In: Environmental Footprints and Eco-Design of Products and Processes*. Springer. pp. 19–43. https://doi.org/10.1007/978-981-10-0655-5_2
- Shi Q, Yu K, Kuang X, Mu X, Dunn CK, Dunn ML, Wang T, Qi HJ (2017) Recyclable 3D printing of vitrimer epoxy. *Mater Horiz* 4(4):598–607. <https://doi.org/10.1039/c7mh00043j>
- Sommerhuber PF, Wenker JL, Rüter S, Krause A (2017) Life cycle assessment of wood-plastic composites: analysing alternative materials and identifying an environmentally sound end-of-life option. *Resour Conserv Recycl* 117:235–248. <https://doi.org/10.1016/j.resconrec.2016.10.012>
- Sutton JT, Rajan K, Harper DP, Chmely SC (2018) Lignin-containing photoactive resins for 3D printing by stereolithography. *ACS Appl Mater Interfaces* 10(42):36456–36463. <https://doi.org/10.1021/acsami.8b13031>
- Tanaka T, Ito H (2013) Manufacturing and processing methods of bio-composites. *In: Polymer Composites*. Wiley. pp. 179–211. <https://doi.org/10.1002/9783527674220.ch5>
- van Voorn B, Smit HHG, Sinke RJ, de Klerk B (2001) Natural fibre reinforced sheet moulding compound. *Compos Part A Appl Sci Manuf* 32(9):1271–1279. [https://doi.org/10.1016/S1359-835X\(01\)00085-9](https://doi.org/10.1016/S1359-835X(01)00085-9)
- Vidakis N, Petousis M, Michailidis N, Kechagias JD, Mountakis N, Argyros A, Boura O, Grammatikos S (2022) High-performance medical-grade resin radically reinforced with cellulose nanofibers for 3D printing. *J Mech Behav Biomed Mater* 134:105408. <https://doi.org/10.1016/j.jmbbm.2022.105408>
- Wang X, Jiang M, Zhou Z, Gou J, Hui D (2017) 3D printing of polymer matrix composites: a review and perspective. *Compos Part B Eng* 110:442–458.

- <https://doi.org/10.1016/j.compositesb.2016.11.034>
- Yang TH, Leu SY, Yang TH, Lo SF (2012) Optimized material composition to improve the physical and mechanical properties of extruded wood-plastic composites (WPCs). *Constr Build Mater* 29:120-127. <https://doi.org/10.1016/j.conbuildmat.2011.09.013>
- Yao J, Hakkarainen M (2023) Methacrylated wood flour-reinforced "all-wood" derived resin for digital light processing (DLP) 3D printing. *Compos Commun* 38. <https://doi.org/10.1016/j.coco.2023.101506>
- Youngquist JA, Myers GE, Muehl JH, Krzysik AM, Clemens CM (1994) Project summary: composites from recycled wood and plastics.
- Zhang S, Bhagia S, Li M, Meng X, Ragauskas AJ (2021) Wood-reinforced composites by stereolithography with the stress whitening behavior. *Mater Des* 206. <https://doi.org/10.1016/j.matdes.2021.109773>
- Zhang S, Li M, Hao N, Ragauskas AJ (2019) Stereolithography 3D printing of lignin-reinforced composites with enhanced mechanical properties. *ACS Omega* 4(23):20197–20204. <https://doi.org/10.1021/acsomega.9b02455>